

We are IntechOpen, the world's leading publisher of Open Access books Built by scientists, for scientists

6,900

Open access books available

186,000

International authors and editors

200M

Downloads

Our authors are among the

154

Countries delivered to

TOP 1%

most cited scientists

12.2%

Contributors from top 500 universities



WEB OF SCIENCE™

Selection of our books indexed in the Book Citation Index
in Web of Science™ Core Collection (BKCI)

Interested in publishing with us?
Contact book.department@intechopen.com

Numbers displayed above are based on latest data collected.
For more information visit www.intechopen.com



Fundamental Models for the Creep of Metals

Rolf Sandström

Additional information is available at the end of the chapter

<http://dx.doi.org/10.5772/intechopen.70726>

Abstract

Analysis of creep properties has traditionally been made with empirical methods involving a number of adjustable parameters. This makes it quite difficult to make predictions outside the range of the original data. In recent years, the author has formulated basic models for prediction of creep properties, covering dislocation, particle and solid solution hardening. These models do not use adjustable parameters. In the present chapter, these models are further developed and utilised. The dislocation mobilities play an important role. The high-temperature climb mobility is extended to low temperatures by taking vacancies generated by plastic deformation into account. This new expression verifies the validity of the combined climb and glide mobility that has been used so far. By assuming that the glide rate is controlled by the climb of the jogs, a dislocation glide mobility is formulated. The role of the mobilities is analysed, and various creep properties are derived. For example, secondary creep rates and strain versus time curves are computed and show good agreement with experimental data.

Keywords: creep, dislocation, mobility, model, creep strain

1. Introduction

If metals are exposed to load at high temperatures, a slow deformation called creep takes place. A characteristic feature of creep is that it occurs even when the load is kept constant. This should be contrasted to plastic deformation at ambient temperatures where an increase in the load is needed to generate further plastic strain. Creep in metals has been studied for many decades, and a number of excellent textbooks exist on the subject, see for example [1–4]. A common way of measuring the creep deformation is to apply a fixed load to a specimen and then record its elongation as a function of time. The relative increase in the elongation is referred to as the (creep) strain. Its time derivative is called the creep strain rate. Another important quantity is the stress, i.e. the load divided by the specimen cross section. After sufficient test time, the specimen ruptures. The rupture time and the specimen elongation at rupture are recorded.

A creep test typically shows three stages: primary, secondary and tertiary. During the primary stage, the creep rate is initially high but shows a gradual decrease until it reaches a constant value, which corresponds to the secondary stage. This stage usually takes the longest time. Finally, the creep rate starts to increase. This is the tertiary stage that eventually leads to rupture. The dependence of the creep strain as a function of time is referred to as a creep (strain) curve. Although the described shape of the creep curve is the most common one, there are many variants.

Creep-exposed materials can be found in many types of high-temperature plants, for example, fossil-fired power plants. The desire is to make the materials as strong as possible, and the creep rate low to ensure a long lifetime. The deformation rate is controlled by the movement of the dislocations, i.e. the line defects that are present in large numbers. If the movement of the dislocations is fast, the creep strength is low. To increase the creep strength, the movement of the dislocations must be reduced. Typically, the most efficient way to hinder this movement is to have a high content of other (forest) dislocations. There is a strong interaction between different dislocations. The second most used way of increasing the strength is to introduce particles in the microstructure. Particles or precipitates are a very potent way of raising the strength. A third way is to have elements in solid solution. The difference in size between the solute and the matrix atoms makes it more difficult for the dislocations to move.

Most creep investigations concern metals above half the melting point. The stress dependence of the strain rate in the secondary stage has always generated much interest in creep research because it has been assumed to reflect the operating dislocation mechanism. In **Figure 1**, such dependence is illustrated for 0.5Cr0.5Mo0.25V steel at 565°C over a wide range of stresses.

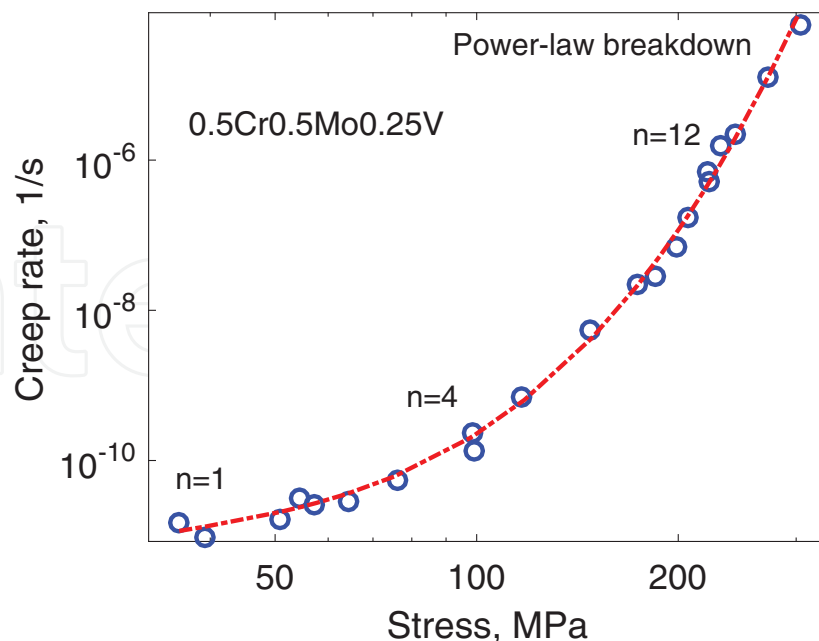


Figure 1. Creep rate versus stress for 0.5Cr0.5Mo0.25V steel at 565°C. The n values indicate the exponent in the power-law creep law. At large stresses, the creep rate increases exponentially with the stress. This is referred to as power-law breakdown. Some of the data points are extrapolated. (After Wilshire [5].)

The slope of the curve is the creep exponent n . At intermediate stresses (and temperatures), the creep exponent is typically in the range 3–8. In the figure, it is 4. At high stresses (and at low temperatures), the creep exponent is much higher, in the figure illustrated with $n = 12$. At still higher stresses, the creep rate varies exponentially with stress, which is called power-law breakdown. At very low stresses, the n value is small, sometimes approaching unity. 0.5Cr0.5Mo0.25V steel is clearly a particle-strengthened material. Other particle-strengthened alloys can show much higher creep exponents than in **Figure 1**.

In the past, the creep exponent has often been used to identify the operating dislocation mechanisms. For intermediate exponents (3–8), climb of dislocations is in general considered as the operating mechanisms although glide has also been assumed for certain alloy types. This will be discussed below. At high stresses, glide has been suggested as the dominating mechanism. At low creep exponents approaching unity, diffusion creep has been assumed as the main mechanism. The consistent change of operating mechanism with stress has been challenged, see for example [5].

In recent years, basic creep models have been formulated. With the help of these models, the assumptions mentioned above will be reanalysed in the present chapter.

2. Dislocation model

To understand the creep process, the key quantity is the dislocation density and its variation with time. Models for the dislocation density development during creep have been available for a long time [6]. Recently, these models have been expanded and derived more precisely. We will use the following formulation [7]:

$$\frac{d\rho}{d\varepsilon} = \frac{m}{bc_L} \rho^{1/2} - \omega\rho - 2\tau_L M \rho^2 / \dot{\varepsilon} \quad (1)$$

where ρ is the dislocation density, ε the strain, m the Taylor factor, b the Burgers vector, τ_L the dislocation line tension, M the dislocation mobility and $\dot{\varepsilon}$ the strain rate. The value of the dislocation mobility M will be discussed below. The dynamic recovery parameter ω for pure metals and the work-hardening constant c_L are given by the following expressions [8, 9]:

$$\omega = \frac{m}{b} d_{\text{int}} \left(2 - \frac{1}{n_{\text{slip}}} \right) \quad (2)$$

$$c_L = \frac{m^2 \alpha G}{\omega (R_m - \sigma_y)} \quad (3)$$

where d_{int} is the interaction distance between dislocations where dislocations of opposite sign get close enough to annihilate each other and thereby reduce the dislocation content. This distance is taken as the core diameter of the dislocations. n_{slip} is the number of active slip systems, which is 12 for fcc alloys. α is a constant in the Taylor equation, G is the shear modulus and R_m and σ_y are the true tensile strength and yield strength at ambient temperatures.

According to Eqs. (2) and (3), ω and c_L are temperature-independent constants. This is also in close agreement with experiments [7, 9]. In some papers, ω has been found to be temperature dependent [10, 11]. However, in these cases the final term in Eq. (1), the static recovery term, has not been considered, which should cover at least part of the temperature dependence. Eq. (1) can be considered as a basic equation for the development of the dislocation density. A detailed derivation of Eq. (1) can be found in [8].

Eq. (1) describes the development of the dislocation density with strain. The first term on the right-hand side is responsible for the generation of dislocations, i.e. work hardening. The two other terms take into account the annihilation of dislocations. The second term gives a strain-controlled recovery, which is called dynamic recovery. The final term is referred to as static recovery. It is time controlled since the strain rate appears in the denominator. The terminology of recovery is not consistent in the literature, which one has to be aware of.

3. Dislocation mobilities

3.1. Climb mobility

The dislocation mobility M in Eq. (1) is an important quantity. It describes the speed v of the dislocations:

$$v = Mb\sigma \quad (4)$$

where σ is the applied stress. Dislocations can propagate by glide along their slip system or by climb perpendicular to the slip system. The latter process requires emission or absorption of atoms by diffusion, and it is slower than glide. The climb mobility at high temperatures ($>0.4 T_m$ where T_m is the melting temperature) was derived by Hirth and Lothe [12]:

$$M_{\text{climb}} = \frac{D_{s0}b}{k_B T} e^{\frac{v\sigma^3}{k_B T}} e^{-\frac{Q}{R_G T}} \quad (5)$$

where T is the absolute temperature, σ the applied stress, D_{s0} the pre-exponential coefficient for self-diffusion, Q the activation energy for self-diffusion, k_B Boltzmann's constant and R_G the gas constant.

At lower temperatures, the climb rate is influenced by the generation of vacancies due to plastic deformation. A brief derivation of this effect will be given here since it cannot be found in the literature. When a climbing dislocation is forced to move, it will emit or absorb vacancies. When gliding dislocations cut each other, jogs in the form of steps of the length of a Burgers vector are formed on them. The jogs are often sessile and must then climb when they move and hence emit or absorb vacancies.

Mecking and Estrin [13] have estimated the number of vacancies produced mechanically in a unit volume per unit time as:

$$P = 0.5 \frac{\sigma \dot{\epsilon}}{Gb^3} \quad (6)$$

The quantities in this equation have been defined above. In [13] the constant in Eq. (6) was estimated to 0.1. A detailed derivation shows that it is 0.5. The annihilation rate A for the excess vacancies was found to be

$$A = \frac{D_{vac}}{\lambda^2} (c - c_0) \quad (7)$$

where c_0 is the equilibrium vacancy concentration and $\Delta c = c - c_0$ is the excess concentration. D_{vac} is the diffusion constant for the vacancies. λ is the spacing between vacancy sinks. Assuming the presence of a substructure, λ can be related to the cell or subgrain size d_{sub} [13], which in turn can be found from the applied stress:

$$\lambda = d_{sub} = \frac{K_{sub}Gb}{\sigma} \quad (8)$$

where K_{sub} is a constant that typically takes values from 10 to 20. From Eqs. (6)–(8), we find the following expression for the excess vacancy concentration:

$$\frac{\Delta c}{c_0} = 0.5 \frac{\sqrt{2}K_{sub}^2 \dot{\epsilon} b^2 G}{D_{self} \sigma} \quad (9)$$

In deriving Eq. (9), we have also made use of a relation for the self-diffusion coefficient:

$$D_{self} = c_0 \Omega D_{vac} \quad (10)$$

where Ω is the atomic volume. It is now assumed that the climb rate is proportional to the total vacancy concentration. This is the same assumption as was made in [13]. The increase in the climb rate g_{climb} due to the presence of excess vacancy concentration from Eq. (10) is then

$$g_{climb} = 1 + \frac{\Delta c}{c_0} \quad (11)$$

To find the total climb mobility, the expression in Eq. (5) should be multiplied by g_{climb} :

$$M_{climb\ enh} = M_{climb} g_{climb} \quad (12)$$

3.2. The glide mobility

In a dislocation-free crystal, the glide mobility is very high. Edington measured a mobility of $M_0 = 1 \times 10^4$ 1/Pa/s for a copper single crystal [14]. In an alloy where a forest of dislocations is present, the mobility is much lower. During deformation as described above, jogs will be formed on the dislocation. Many times the jogs have to move perpendicular to their glide planes. This means that they are sessile, i.e. they have to move by

climb [12], which is a slow process. It is natural to assume that it is the motion the jogs that controls the glide rate and that is what we will do. This is also what Hirth and Lothe have assumed [12].

The basis for the glide mobility is Eq. (12), since the jogs move by climb. However, there is an additional factor. Only a small fraction of each dislocation consists of jogs. Since the jogs move slowly, the forces on the dislocations are concentrated to the jogs. The average distance between jogs can be determined from the dislocation density ρ as $l_{\text{jog}} = 1/\sqrt{\rho}$. The force F on a dislocation is given by the Peach-Koehler formula $F = b \sigma l$ where l is the length of the dislocation. If l is chosen as l_{jog} , F will be the force on each jog. Consequently, the stress on the jogs is increased by

$$g_{\text{glide}} = \frac{l_{\text{jog}}}{b} = \frac{1}{b\sqrt{\rho}} \quad (13)$$

where the length of a jog is taken as the length of the Burgers vector. With the help of Taylor's equation,

$$\sigma = \sigma_y + \alpha m G b \sqrt{\rho} \quad (14)$$

where σ_y being the yield strength, Eq. (13) can be rewritten as

$$g_{\text{glide}} = \frac{\alpha m G}{\sigma - \sigma_y} \quad (15)$$

The glide mobility is obtained by multiplying the climb mobility by g_{glide} :

$$M_{\text{glide}} = M_{\text{climb}} g_{\text{climb}} g_{\text{glide}} \quad (16)$$

Eq. (16) applies to both edge and screw dislocations. With the assumptions considered, the climb and glide mobility are closely related. g_{glide} is roughly equal to the ratio between the shear modulus G and the applied stress σ . Since G is much larger than σ , g_{glide} is always significantly larger than unity. Thus, the glide mobility is larger than the climb mobility, which is a common assumption when modelling creep.

3.3. Cross slip mobility

Screw dislocations can change glide plane with the help of cross slip. This can simplify the annihilation of dislocations with opposite signs and thereby contribute to the recovery. Cross slip requires an additional activation energy E_{cs} . Püschl gave the following estimate of E_{cs} [15]:

$$E_{\text{cs}} = 0.012 G b^3 \frac{d_{\text{SFE}}}{b} \ln \left(\frac{2d_{\text{SFE}}}{b} \right) \quad (17)$$

where d_{SFE} is the width of a stacking fault [12]:

$$d_{SFE} = \frac{Gb^2}{8\pi\gamma_{SFE}} \frac{(2 - \nu_P)}{(1 - \nu_P)} \quad (18)$$

where ν_P is Poisson's ratio and γ_{SFE} is the stacking-fault energy. With stacking-fault energies of 45 mJ/m² for copper and 166 mJ/m² for aluminium [16], the resulting values for E_{cs} become 560 and 40 kJ/mol, respectively. Thus, a pronounced temperature dependence is obtained. Eq. (17) is based on elasticity theory models. However, recently ab initio calculations have been performed providing similar results to those of Eq. (17) [17, 18]. Now, the influence of cross slip on the mobility can be introduced:

$$g_{cross-slip} = \exp\left(-\frac{E_{cs}}{R_G T}\right) \quad (19)$$

$$M_{cross-slip} = M_{climb} g_{climb} g_{glide} g_{cross-slip} \quad (20)$$

The consequences of the strong temperature dependence in the model for cross slip mobility will be discussed later in Section 6.

3.4. The climb-glide mobility

The results in Sections 3.1–3.3 are new. It has been recognised that the climb mobility in Eq. (5) predicted far too low creep rates at low temperatures and high stresses. It was thought that glide could be the controlling mechanism during these conditions. For this purpose, a combined climb and glide mobility was introduced [19]:

$$M_{clglide} = M_{climb} f_{clglide} \quad (21)$$

where $f_{clglide}$ is given by

$$f_{clglide} = \exp\left(\frac{Q}{R_G T} \left(\frac{\sigma}{R_{max}}\right)^2\right) \quad (22)$$

where R_{max} is the true tensile strength at ambient temperatures. Eq. (22) has several important consequences at low temperatures. First, it reduces the activation energy for creep. Second, it increases the creep rate by a large factor. Third, it raises the value of the creep exponent dramatically. These results are in excellent agreement with experiments [9, 20]. Examples will be given below in Sections 4 and 5.

The derivation of Eq. (21) was inspired by the work of Kocks et al. [21]. They gave an empirical expression for the glide mobility. Unfortunately, it involved five unknown parameters and was therefore of little use directly. However, some of the parameters could be fixed by following a procedure due to Nes where an integrated climb and glide mobility was formulated [22]. The remaining parameters could be set with the help of work by Chandler [23].

Ideally, to describe creep, the fundamental models for the mobilities derived in Sections 3.1–3.3 should be used. However, they are difficult to use directly since g_{climb} involves the strain rate.

Instead, the equations in Sections 3.1–3.3 will be used to verify Eq. (22), which can then be applied to derive the creep rate. Direct comparison between g_{climb} and f_{clglide} is shown in Figures 2 and 3 for aluminium.

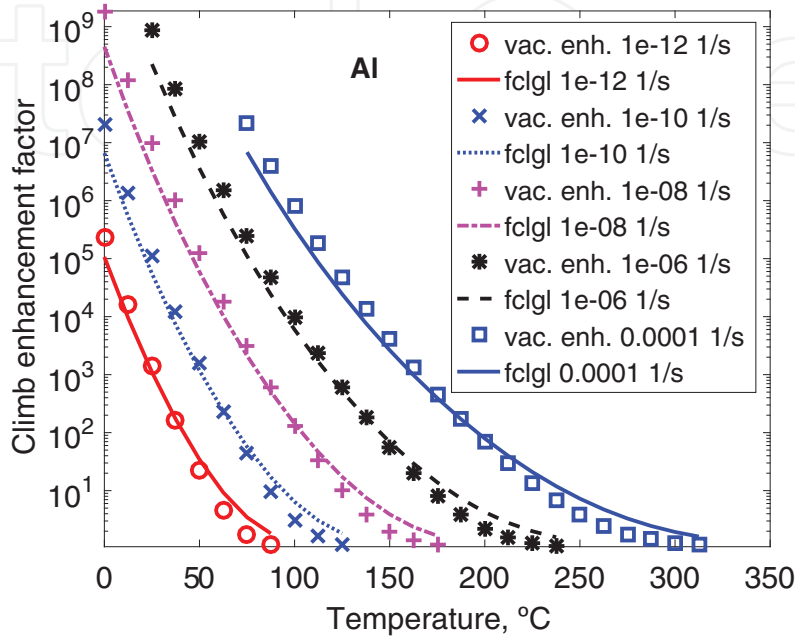


Figure 2. Climb enhancement factor versus temperature at five strain rates for aluminium. Eq. (11), for the increase in vacancy concentration due to plastic deformation, is compared with Eq. (22) for the climb-glide enhancement.

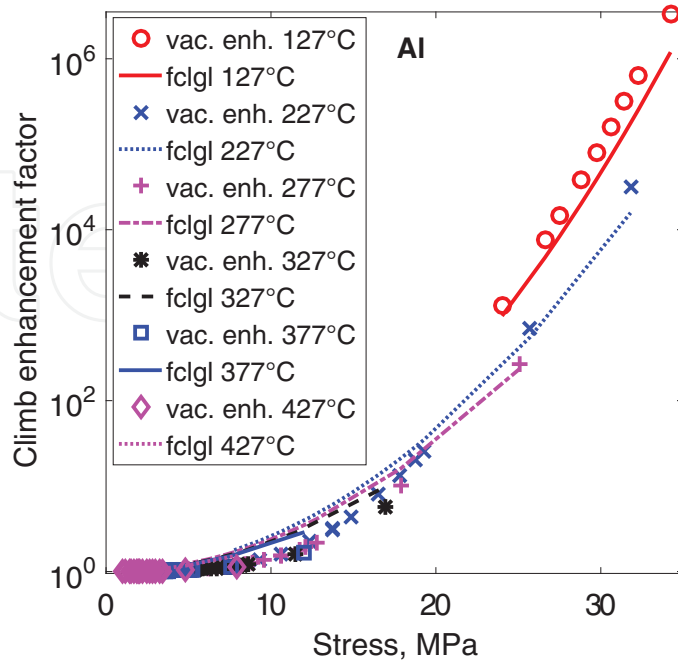


Figure 3. Climb enhancement factor versus stress at six temperatures for aluminium. Eq. (11) is compared with Eq. (22). The values of stresses and strain rates are taken from experimental creep data [24].

In **Figure 2**, a continuous set of parameters for temperature and strain rate are used, whereas in **Figure 3** experimental values are applied. It can be seen that the enhancement in vacancy concentration due to plastic deformation can fully explain the increase in creep rate in relation to the high-temperature climb mobility.

A second example of the comparison is given in **Figure 4** for copper.

Again the agreement between the two sets of models is quite good. The temperature, stress and strain rate dependences are well covered in **Figures 2–4**.

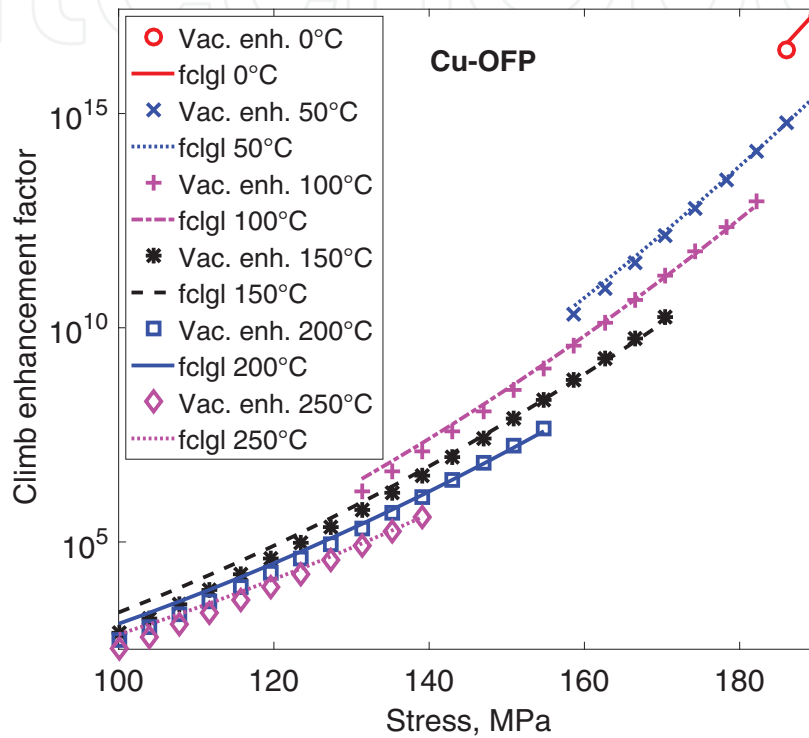


Figure 4. Climb enhancement factor versus stress at six temperatures for Cu-OFP. Eq. (11) for the increase in vacancy concentration due to plastic deformation is compared with Eq. (22) for the climb-glide enhancement.

4. Secondary creep

4.1. Pure elements

Our understanding of the creep process is largely based on the creep recovery theory [6]. The key feature of this theory is that the recovery rate is sufficiently rapid that the dislocation density can be kept constant during secondary creep. If the dislocation density is continuously rising, the creep deformation will slow down and eventually stop, which is contrary to observations. Thus, there is a balance between the generation and the annihilation of dislocations during creep. If we assume stationary conditions, the strain derivative in Eq. (1) vanishes. The resulting expression for secondary strain rate is

$$\dot{\epsilon}_{\text{sec}} = 2\tau_L M \rho^{3/2} / \left(\frac{m}{bc_L} - \omega \rho^{1/2} \right) \quad (23)$$

Using Taylor's Eq. (14), Eq. (23) can be expressed in terms of stresses:

$$\dot{\epsilon}_{\text{sec}} = h(\sigma - \sigma_i) \quad \text{with} \quad h(\sigma) = 2\tau_L M(T, \sigma) \frac{\sigma^3}{(\alpha m G b)^3} / \left(\frac{m}{b c_L} - \omega \frac{\sigma}{\alpha m G b} \right) \quad (24)$$

$$\sigma_{\text{disl}} = \alpha m G b \rho^{1/2} = \sigma - \sigma_i \quad (25)$$

where σ_{disl} is the dislocation stress. σ_i is an internal stress that can have contributions from the yield strength, solid solution hardening and particle hardening. At low stresses, the mobility M is given by Eq. (5) that is independent of stress. If no internal stress is present, Eq. (24) gives an approximate power-law expression with a stress exponent of 3. Such a stress exponent is often observed at high temperatures for austenitic stainless steels [25].

With our present knowledge, the natural assumption is that static recovery is controlled by climb. This is analysed in Section 6. This means that it is the climb mobility in Eq. (12) that should be used in Eq. (24). In addition, we saw in Section 3.4 that the expression for the enhancement factor for the climb mobility g_{climb} due to the raised vacancy concentration in Eq. (11) agreed with the climb-glide enhancement factor f_{clglide} in Eq. (22). Since the implication of f_{clglide} is known to successfully have described experimental data, this gives further support to the use of Eq. (12).

Eq. (24) will now be applied to pure aluminium. For σ_i , the Peierls stress will be used. Although a Peierls stress is not usually considered to be of importance for fcc alloys, recent studies suggest that this conclusion is not true for Al. With ab initio methods, Shin and Carter

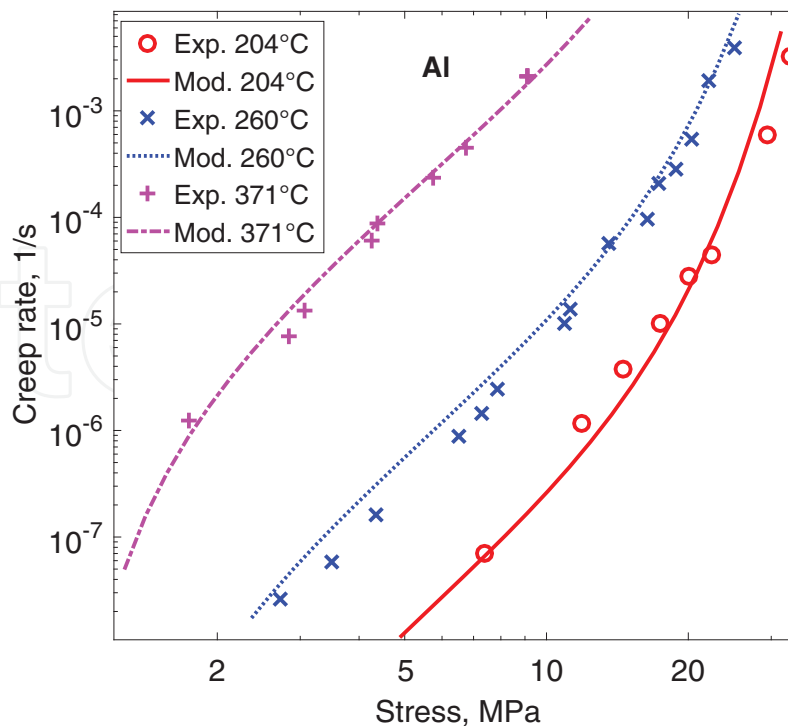


Figure 5. Secondary creep rate versus stress for pure aluminium. Eq. (24) is compared to experimental data from [27].

found the following value for the Peierls stress of edge dislocation σ_{pe} [26]. The value for screw dislocations was much smaller:

$$\sigma_{pe} = 4.9 \times 10^{-5} G \quad (26)$$

The application of Eq. (24) is illustrated in **Figure 5**.

At intermediate stresses in **Figure 5**, the slope of the curves is about 4.5, which is the value of the stress exponent. At higher stresses, the slope increases that is referred to as power-law breakdown. At low stresses, there is also an increase of the stress exponent. This is due to the presence of the internal stress in Eq. (26). It can be seen that the model in Eq. (24) can handle these three regions of the creep rate versus stress curves quite well.

4.2. Solid solution

The presence of elements in solid solution has two effects on the secondary creep rate. It gives rise to a drag stress or a break stress, and it increases the activation energy for creep. The increase in the activation energy is U_j^{\max} , which is the maximum interaction energy between a dislocation and a solute j [28]:

$$U_j^{\max} = \frac{\beta}{b} = \frac{1(1 + \nu_p)}{\pi(1 - \nu_p)} G \Omega_0 \varepsilon_j \quad (27)$$

where Ω_0 is the atomic volume and ε_j the linear lattice misfit of solute j . The additional contribution to the activation energy is taken into account by multiplying the dislocation mobility by the factor f_Q :

$$f_Q = e^{-U_j^{\max}/RT} \quad (28)$$

For slowly diffusing solutes, the contribution to the internal stress, cf. Eq. (24), is the drag stress [28]:

$$\sigma_j^{drag} = \frac{v c_{j0} \beta^2}{b D_j k_B T} I(z_0) \quad (29)$$

where v is the dislocation speed, cf. Eq. (4), c_{j0} is the concentration of solute j and D_j the diffusion constant for solute j . $I(z_0)$ is an integral of $z_0 = b/r_0 k_B T$ where r_0 is the dislocation core radius. $I(z_0)$ often takes values of around 3.

The use of Eq. (29) is illustrated for Al-Mg alloys in **Figure 6**. The drag stress is added to the internal stress in Eq. (24). The factor in Eq. (28) is also taken into account which raises the activation energy for creep by the amount U_j^{\max} , where j refers to Mg.

In the same way as for pure aluminium, there are three stages of stress dependence. In the middle range of stresses, power-law behaviour is obeyed. At low stresses, there is a slight increase in the creep exponent due to the presence of the Peierls stress that is the same as for

pure aluminium. At high stresses, power-law breakdown takes place with an increase in the stress exponent.

The modelling in **Figure 6** is based on the climb mobility, so climb is assumed to be the controlling mechanism over the full-stress range. In the literature, it has frequently been assumed that glide is controlling in the middle stress range, see for example [31]. This should be due to a larger effect of solid solution hardening on gliding than on climbing dislocations. This is difficult to understand, since solid solution hardening has about the same effect for both mechanisms [32]. In addition, why there should be transitions in mechanism at low and high stresses is not obvious. Sometimes, it is assumed that the solutes break away from the dislocations at high stresses, but that is predicted to take place at much higher stresses than where the transition takes place [12]. Considering glide as a controlling mechanism is not consistent with the glide mobility in Eq. (16). If that is applied, the experimental results in **Figure 6** cannot be reproduced.

For fast diffusion elements such as interstitials, the drag stress according to Eq. (29) is usually negligibly small. Instead, the solutes are locked to the dislocations, and they have to break away to become mobile. The size of the break stress that should be added to the internal stress σ_i in Eq. (24) is given by [28, 32]

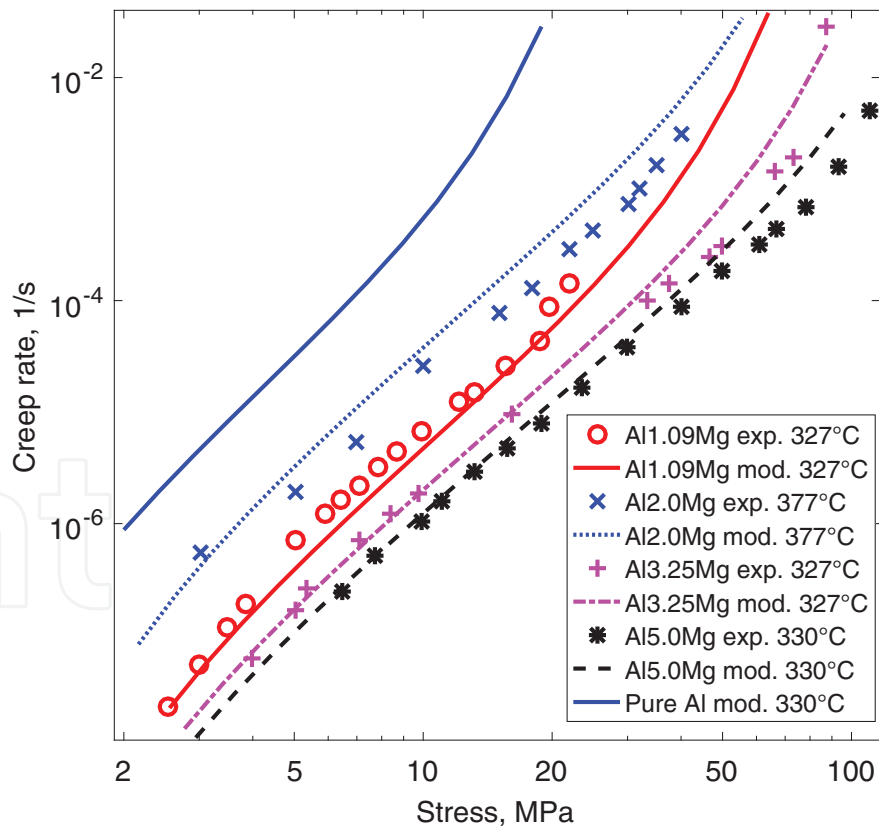


Figure 6. Secondary creep rate versus stress for Al-Mg alloys. Eq. (24) with the stress contribution to the internal stress from Eq. (29) and the increase in activation energy from Eq. (28) is compared to experimental data [29–31].

$$\sigma_{j_{\text{break}}} = \frac{U_j^{\text{max}} c_{j0}}{b^3} \int_{y_L}^{y_R} e^{-\frac{W_j(y)}{kT}} dy \quad (30)$$

The break stress is proportional to U_j^{max} . $W_j(y)$ is the interaction energy between a solute j and a dislocation at a distance y . The integration is performed over a distance of about $\pm 20 b$. The application of Eq. (30) is illustrated for copper with 100 at. ppm phosphorus (Cu-OFP). At low temperatures, phosphorus gives a strong improvement of the creep strength. The solute phosphorus has two effects. It increases the creep activation energy by U_j^{max} , and a break stress is added to the internal stress in Eq. (24). The result is shown in **Figure 7** for oxygen-free copper (Cu-OF) with and without phosphorus.

From **Figure 7**, it is obvious that the model can describe the influence of phosphorus on the creep rate quantitatively. No adjustable parameters are used in this figure (or in any other figure in the chapter). For Cu-OFP the creep exponent is about 65 in **Figure 7**. This demonstrates the validity of Eq. (24) also deep down in the power-law breakdown regime.

4.3. Stress-strain relations

Handling of stress-strain curves is not the subject of this chapter. The only message is that Eq. (1) can also be used to predict stress-strain curves. For further details, the reader is referred to [7, 33].

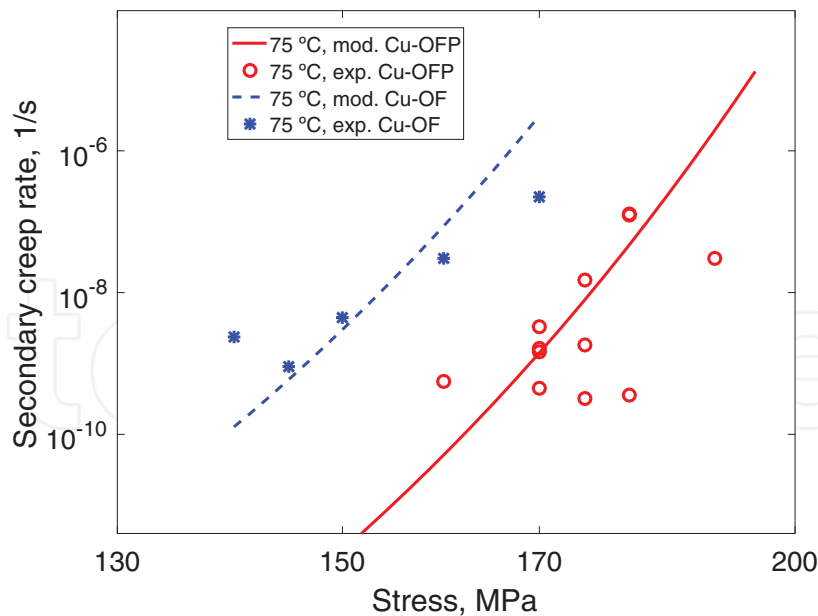


Figure 7. Secondary creep rate versus stress for oxygen-free copper with and without phosphorus at 75°C. Eq. (24) with the stress contribution to the internal stress from Eq. (30) and the increase in activation energy from Eq. (28) is compared to experimental data. After [28].

5. Creep strain curves

In the primary stage, the creep rate is in most cases larger than in the secondary stage. This is assumed to be due to a lower dislocation density and thereby a lower dislocation stress. The additional driving stress during primary creep becomes [34]

$$\sigma_{\text{primadd}} = \sigma_{\text{dislstat}} - \sigma_{\text{disl}} \quad (31)$$

where σ_{dislstat} is the dislocation density during stationary conditions, which is given by the difference between the applied stress σ and the internal stress σ_i :

$$\sigma_{\text{dislstat}} = \sigma - \sigma_i \quad (32)$$

The total stress during primary creep is given by

$$\sigma_{\text{prim}} = \sigma + \sigma_{\text{primadd}} = 2\sigma - \sigma_{\text{disl}} - \sigma_i \quad (33)$$

where Eqs. (31) and (32) have been inserted. Eq. (33) gives the stress that should be used in the expression for the secondary creep rate (Eq. (24)) to obtain the general expression for the creep rate:

$$\dot{\epsilon}(\sigma) = \dot{\epsilon}_{\text{sec}}(2\sigma - \sigma_{\text{disl}} - \sigma_i) \quad (34)$$

When the secondary stage is reached, $\sigma = \sigma_i + \sigma_{\text{disl}}$ and $\dot{\epsilon}(\sigma)$ are equal to the secondary creep rate, according to Eq. (24) as it should. When σ_{disl} is smaller than its stationary value, the creep rate is higher, which is characteristic for primary creep. The use of Eq. (34) is illustrated in **Figure 8**. In **Figure 8a**, a creep strain versus time curve is shown for Cu-OFP. The creep rate versus time for the same case is given in **Figure 8b**. In the double logarithmic diagram, a straight line is obtained, which is in close agreement with the experimental data. This type of relation that is referred to as the φ model is quite frequently observed. It has several different

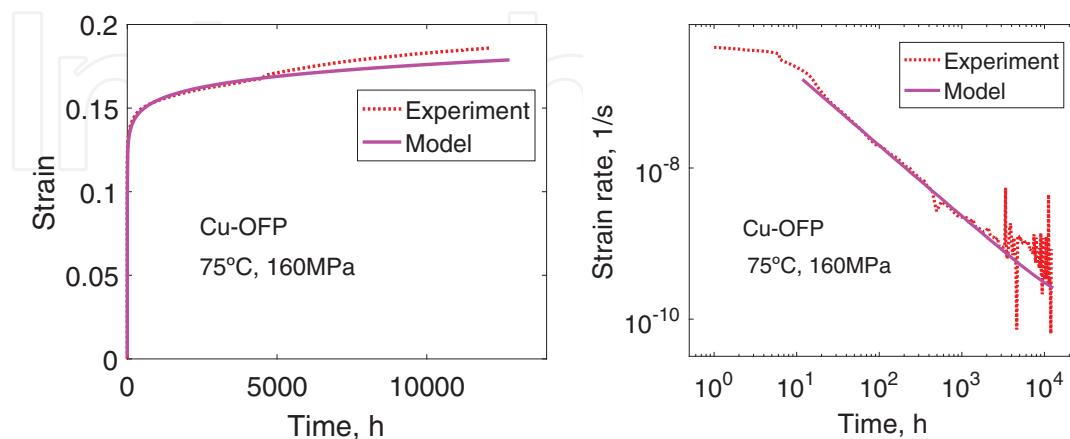


Figure 8. Creep strain results according to Eq. (34) are compared to experimental data for Cu-OFP at 75°C and 160 MPa: (a) creep strain versus time and (b) creep rate versus time. After [34]. The cusps on this curve are due to the necessity of reloading the specimen after a certain strain.

names [9]. It is most well known for 9% Cr steels, see for example [35]. It is evident that Eq. (34) can describe primary creep quite well.

6. Creep recovery theory

At ambient temperatures, for example, in steels, a gradually decreasing creep rate is observed at constant load until the deformation in practice stops completely. This is known as logarithmic creep. In constant strain rate tests, the deformation increases as long as the load is increasing. This behaviour takes work hardening and dynamic recovery into account but not static recovery. The derivation of the expression for the dynamic recovery constant is based on pure glide [36]. It has been suggested many times in the literature that dynamic recovery is controlled by cross slip, see for example [15, 37]. Qualitatively, this might seem logically. Cross slip allows the screw dislocations to annihilate each other, leading to the partial recovery that is characteristic for deformation processes at ambient temperatures in steels. The problem is that the available models for cross slip that were summarised in Section 3.3 give temperature dependencies that are orders of magnitude larger than the observed ones. Unfortunately, we must conclude that we do not understand the role of cross slip at present. In fact, we can model observed dynamic recovery considering just glide.

Most measured creep curves are characterised by a primary, a secondary and a tertiary stage. Work hardening and recovery are continuously taking place. According to the creep recovery theory, there is balance between work hardening and recovery in the secondary stage. Otherwise, there would be either a raise or a decrease in the dislocation density, giving a reduction or increase in the creep rate, respectively. Consequently, the dislocation density must remain approximately unchanged in the secondary stage.

At high temperatures ($T > 0.5 T_m$), there is consensus that static recovery is controlled by climb in so-called class II alloys, which include most creep-exposed alloys of technical interest. This mechanism allows dislocations of opposite sign that attract each other to move towards each other and finally annihilate. On the other hand, in class I alloys, glide has been assumed to be controlling in a certain stress range with a creep exponent of 3. The most well-known type of alloy in this class is AlMg. The assumption is problematic for several reasons. (i) The reason for glide control is considered to be strong solid solution hardening. However, the effect of solid solution hardening is almost equally strong for climb [28, 32]. In addition, the glide rate is always faster than the climb rates according to Eqs. (12) and (16). (ii) At the upper end of the stress range with a creep exponent of 3, break-away of solutes from the dislocations is assumed to take place. The models for this effect suggest a much higher stress than the one observed. (iii) The most problematic issue is that the static recovery must be based on glide. From observations at ambient temperatures, it is unlikely to be possible. An alternative approach was presented in Section 4.2 fully based on a climb model. It was demonstrated that all the mentioned issues could be solved. In addition, a good fit to the data was found.

At or close to ambient temperatures, several metals give creep curves that have the same general appearance as at high temperatures ($T > 0.5 T_m$) with primary, secondary and tertiary

creep. For example, this is the case for Cu-OFP, see **Figure 8**. For a long time, it was assumed that creep was controlled by glide and cross slip at low temperatures [19], because the estimated climb rate was much too low to be of importance. However, this is not considered to be the case anymore. When taking the enhanced vacancy concentration into account, the observed creep rates for copper and aluminium can be fully explained by climb. This is evident from **Figure 7**. In addition, it clarifies why static recovery can take place at low temperatures, which is very difficult assuming the presence of only glide and cross slip.

7. Conclusions

- To model creep of alloys, the development of the dislocation density must be known. In recent years, a basic model for the dislocation density has been formulated that fulfils this requirement. Together with models for solid solution and particle hardening, the creep behaviour of many alloys can be described without the use of adjustable parameters.
- A new expression for the dislocation climb mobility has been derived. It extends the well-established formula of Hirth and Lothe to lower temperatures by taking the enhanced concentration of vacancies due to plastic deformation into account. The new expression can explain observed creep rates down to near-ambient temperatures.
- Assuming that glide of dislocations is controlled by the climb rate of their jogs, an expression for the dislocation glide mobility is formulated. It turns out that the glide rate is always higher than the climb rate. This suggests that climb is rate controlling in dislocation creep. In the chapter, it is illustrated for AlMg alloys that this might apply to class I alloys as well.
- It is suggested in the literature that cross slip is the controlling mechanism for dynamic recovery. An expression for the cross slip mobility is set up based on published models for the activation energy of cross slip. However, this expression cannot explain the observed rate of dynamic recovery. This is still only possible by assuming glide control.
- It is demonstrated that the dislocation model can describe a range of properties without the use of adjustable parameters. These properties include secondary creep and stress-strain curves.

Author details

Rolf Sandström

Address all correspondence to: rsand@kth.se

Materials Science and Engineering, KTH Royal Institute of Technology, Stockholm, Sweden

References

- [1] Evans RW, Wilshire B. Creep of Metals and Alloys. Institute of Metals, London; 1985
- [2] Penny RK, Marriott DL. Design for Creep. Chapman & Hall, London; 1995
- [3] Abe F, Kern T-U, Viswanathan Eds R. Creep-Resistant Steels. Woodhead, Cambridge; 2008
- [4] Kassner ME. Fundamentals of Creep in Metals and Alloys. Butterworth-Heinemann, Oxford; 2015
- [5] Wilshire B. Observations, theories, and predictions of high-temperature creep behavior. Metallurgical and Materials Transactions A: Physical Metallurgy and Materials Science. 2002;**33**:241-248
- [6] Lagneborg R. Dislocation mechanisms in creep. International Metallurgical Reviews. 1972;**17**:130-146
- [7] Sandström R, Hallgren J. The role of creep in stress strain curves for copper. Journal of Nuclear Materials. 2012;**422**:51-57
- [8] Sandström R. The role of microstructure in the prediction of creep rupture of austenitic stainless steels. In: ECCC Creep & Fracture Conference; Düsseldorf; 2017
- [9] Sandstrom R. Basic model for primary and secondary creep in copper. Acta Materialia. 2012;**60**:314-322
- [10] Kocks UF. Laws for work-hardening and low-temperature creep. Journal of Engineering Materials and Technology, Transactions of the ASME. 1976;**98**:76-85
- [11] Hallén H. A theory of dynamic recovery in F.C.C. metals. Materials Science and Engineering. 1985;**72**:119-123
- [12] Hirth JP, Lothe J. Theory of Dislocations. Malabar, Florida: Krieger; 1982
- [13] Mecking H, Estrin Y. The effect of vacancy generation on plastic deformation. Scripta Metallurgica. 1980;**14**:815-819
- [14] Edington JW. The influence of strain rate on the mechanical properties and dislocation substructure in deformed copper single crystals. Philosophical Magazine. 1969;**19**:1189-1206
- [15] Püschl W. Models for dislocation cross-slip in close-packed crystal structures: A critical review. Progress in Materials Science. 2002;**47**:415-461
- [16] Wu X-Z, Wang R, Wang S-F, Wei Q-Y. Ab initio calculations of generalized-stacking-fault energy surfaces and surface energies for FCC metals. Applied Surface Science. 2010;**256**: 6345-6349
- [17] Du J-P, Wang C-Y, Yu T. Cross-slip process in model Ni(Al) solid solution: An embedded-atom method study. Computational Materials Science. 2014;**91**:192-199

- [18] Nöhring WG, Curtin WA. Dislocation cross-slip in fcc solid solution alloys. *Acta Materialia*. 2017;**128**:135-148
- [19] Sandstrom R, Andersson HCM. Creep in phosphorus alloyed copper during power-law breakdown. *Journal of Nuclear Materials*. 2008;**372**:76-88
- [20] Sandström R. Fundamental models for creep properties of steels and copper. *Transactions of the Indian Institute of Metals*. 2016;**69**:197-202
- [21] Kocks UF, Argon AS, Ashby MF. Thermodynamics and kinetics of slip. *Progress in Materials Science*. 1975;**19**:1
- [22] Nes E, Marthinsen K. Modeling the evolution in microstructure and properties during plastic deformation of f.c.c.-metals and alloys—An approach towards a unified model. *Materials Science and Engineering: A*. 2002;**322**:176-193
- [23] Chandler HD. Effect of unloading time on interrupted creep in copper. *Acta Metallurgica et Materialia*. 1994;**42**:2083-2087
- [24] Mecking H, Styczynski A, Estrin Y. Steady state and transient plastic flow of aluminium and aluminium alloys. In: . *Strength of Metals and Alloys (ICSMA 8)*. Oxford: Pergamon; 1989. p. 989-994
- [25] Vujic S, Sandstrom R, Sommitsch C. Precipitation evolution and creep strength modelling of 25Cr20NiNbN austenitic steel. *Materials at High Temperatures*. 2015;**32**:607-618
- [26] Shin I, Carter EA. Possible origin of the discrepancy in Peierls stresses of fcc metals: First-principles simulations of dislocation mobility in aluminum. *Physical Review B: Condensed Matter and Materials Physics*. 2013;**88**:064106:1-10
- [27] Servi IS, Grant NJ. Creep and stress rupture behaviour of aluminium as a function of purity. *Transactions of AIME*. 1951;**191**:909-916
- [28] Korzhavyi PA, Sandström R. First-principles evaluation of the effect of alloying elements on the lattice parameter of a 23Cr25NiWCuCo austenitic stainless steel to model solid solution hardening contribution to the creep strength. *Materials Science and Engineering A*. 2015;**626**:213-219
- [29] Oikawa H, Honda K, Ito S. Experimental study on the stress range of class I behaviour in the creep of Al-Mg alloys. *Materials Science and Engineering*. 1984;**64**:237-245
- [30] Sato H, Maruyama K, Oikawa H. Effects of the third element on creep behavior of Al-Mg and α Fe-Be solid solution alloys. *Materials Science and Engineering A*. 1997;**234-236**:1067-1070
- [31] Horita Z, Langdon TG. High temperature creep of Al-Mg alloys. In: . *Strength of Metals and Alloys (ICSMA 7)*. Pergamon; 1985. p. 797-802
- [32] Sandstrom R, Andersson HCM. The effect of phosphorus on creep in copper. *Journal of Nuclear Materials*. 2008;**372**:66-75

- [33] Sandström R. Influence of phosphorus on the tensile stress strain curves in copper. *Journal of Nuclear Materials*. 2016;**470**:290-296
- [34] Sandström R. The role of cell structure during creep of cold worked copper. *Materials Science and Engineering: A*. 2016;**674**:318-327
- [35] Abe F. Analysis of creep rates of tempered martensitic 9%Cr steel based on microstructure evolution. *Materials Science and Engineering A*. 2009;**510-511**:64-69
- [36] Roters F, Raabe D, Gottstein G. Work hardening in heterogeneous alloys—A microstructural approach based on three internal state variables. *Acta Materialia*. 2000;**48**:4181-4189
- [37] Jackson PJ. Dislocation modelling of shear in f.c.c. crystals. *Progress in Materials Science*. 1985;**29**:139-175

